Distribution function of nuclei from $e^{\pm}$ scattering in the presence of a strong primordial magnetic field

Motohiko Kusakabe[*]

School of Physics, and International Research Center for Big-Bang Cosmology and Element Genesis,
Beihang University 37, Xueyuan Road, Haidian-qu, Beijing 100083 China

Atul Kedia, Grant J. Mathews, and Nishanth Sasankan

Center for Astrophysics, Department of Physics, University of Notre Dame,
Notre Dame, Indiana 46556, USA

The amplitude of the primordial magnetic field (PMF) is constrained from observational limits on primordial nuclear abundances. Within this constraint, it is possible that nuclear motion is regulated by Coulomb scattering with electrons and positrons ($e^{\pm}$s), while $e^{\pm}$s are affected by a PMF rather than collisions. For example, at a temperature of 10^9 K, thermal nuclei typically experience $\sim 10^{21}$ scatterings per second that are dominated by very small angle scattering leading to minuscule changes in the nuclear kinetic energy of order $\mathcal{O}(1)$ eV. In this paper the upper limit on the effects of a possible discretization of the $e^{\pm}$ momenta by the PMF on the nuclear momentum distribution is estimated under the extreme assumptions that the momentum of the $e^{\pm}$ is relaxed before and after Coulomb scattering to Landau levels, and that during Coulomb scattering the PMF is neglected. This assumption explicitly breaks the time reversal invariance of Coulomb scattering, and the Maxwell-Boltzmann distribution is not a trivial steady state solution of the Boltzmann equation under these assumptions. We numerically evaluate the collision terms in the Boltzmann equation, and show that the introduction of a special direction in the $e^{\pm}$ distribution by the PMF generates no directional dependence of the collisional destruction term of nuclei. Large anisotropies in the nuclear distribution function are then constrained from big bang nucleosynthesis. Ultimately, we conclude that a PMF does not significantly affect the isotropy or big bang nucleosynthesis.

I. INTRODUCTION

In the early Universe, nuclei are strongly coupled with electrons and positrons ($e^{\pm}$) via Coulomb scattering [1,2]. A standard assumption during big bang nucleosynthesis (BBN) is that the nuclear energy distribution obeys Maxwell-Boltzmann (MB) statistics as a nonrelativistic approximation to the Fermi-Dirac (FD) and Bose-Einstein (BE) distribution functions [3,4].

Simulations of nuclear motion in a relativistic $e^{\pm}$ plasma during the BBN epoch have been recently performed with Coulomb scatterings taken into account. It was shown that the rapid thermalization of nuclei leads to an MB distribution [2,5]. A perturbative analysis of the relativistic Boltzmann equation shows that any fractional deviation of the thermal nuclear distribution from the MB distribution is of the order 10^{-18} at a temperature of $T = 1$ GK, limited by the factor of H/Γ_{Coul}, where H is the cosmic expansion rate and Γ_{Coul} is the scattering rate of nuclei [6].

If there is a nonthermal particle source such as decaying exotic particles and evaporating black holes in the early Universe, then high energy tails in the spectra of photons and nuclei can be deformed and the BBN yields could be affected [5,7–9]. Also, the effect of replacing an MB distribution for nuclei with Tsallis distributions [10] has been studied. It was shown that this can change the nuclear reaction rates and primordial abundances [11,12]. Note, however, that if the nuclear distribution functions differ from MB statistics, then the relative velocity distribution depends upon the masses of reacting nuclei in contrast to the case of MB in which it only depends upon the reduced mass [13]. In addition, if the MB statistics is modified to Tsallis statistics, the phase space is changed from the simple product of the distribution functions of reacting particles as prescribed in the standard reaction theory [14].

A possible source of deviation of particle distributions from MB is the existence of a primordial magnetic field (PMF). A strong magnetic field changes weak [15–17] and nuclear [18] reaction rates, as well as thermodynamic properties of the $e^{\pm}$s [18,19] through Landau discretization of the particle momenta. In addition, the PMF energy

*kusakabe@buaa.edu.cn

enhances the cosmic expansion rate [20], and mainly through this effect the PMF is constrained to be $B_0 < 1.5\ \mu$G at present or $B < 2.0 \times 10^{11}$ G at $T_9 \equiv T/(10^9\ \text{K}) = 1$ [18,21]. The BBN constrains PMFs generated earlier in the big bang, i.e., the electroweak phase transition [22], neutrino decoupling [23], and so on. These small-scale PMFs, however, undergo dissipation during the later cosmic evolution [22,24–26]. This PMF evolution depends upon the helicity and homogeneity of the magnetic fields [24,27], and its behavior in the late nonlinear structure formation phase has been investigated in a number of recent three-dimensional simulations [28–31]. Ultimately, what we can observe with current measurements are signatures of large-scale PMFs which could have been generated in the inflationary epoch before the big bang [32]. Constraints on the PMF [26] have been deduced from various astronomical observations such as the CMB temperature and polarization from gravitational [33–39] and heating effects [40], the redshifted 21-cm signal from heating effects [31,41–43], ultrafaint dwarf galaxies from gravitational effects [44], and gravitational waves (at very small scales) [45].

It has been pointed out that an inhomogeneous PMF with a comoving amplitude of $B_0 = \mathcal{O}(0.1)$ nG and a coherence length of $\lambda = \mathcal{O}(10)$ kpc can induce chemical separations of Li^+ ions from gravitationally collapsing cosmic structures [46,47]. As a result, this sub-nG magnetic field could explain the long-standing discrepancy between the Li abundances in metal-poor stars [48,49] and the standard BBN prediction [see Ref. [50] for the latest result based upon recent experiments on the $^7\text{Be}(n, p)^7\text{Li}$ reaction]. Interestingly a PMF with $B_0 = \mathcal{O}(0.1)$ nG over similar scales also induces baryon inhomogeneities before the epoch of cosmological recombination [51], and its effect on the cosmic microwave background (CMB) could also help explain the difference between Hubble parameters deduced from observations of Type Ia supernovae and the CMB [52].

The magnetic field amplitude is also constrained from the CMB power spectra and baryon acoustic oscillation data [53]. The constraint on the number of effective relativistic degrees of freedom is $N_{\text{eff}} = 2.99 \pm 0.17$. This corresponds to $B_0^2 = (-0.13 \pm 0.27)\ \mu\text{G}^2$ in terms of energy density, based upon the relation:

$$B_0^2 \approx \frac{7\pi^3}{15}\left(\frac{4}{11}\right)^{4/3}(N_{\text{eff}} - N_{\text{eff},0})T_0^4,$$
$$= 2.383(N_{\text{eff}} - N_{\text{eff},0})\mu\text{G}^2, \qquad (1)$$

where $N_{\text{eff},0} = 3.046$ is the contribution from three generations of relic neutrinos and antineutrinos, and $T_0 = 2.7255$ K is the present CMB temperature. The 2σ upper limit on the comoving field strength is then $B_0 < 0.82\ \mu$G. However, we caution the reader regarding three points here: (1) since most of the small-scale fields would dissipate during a long cosmic time from the BBN epoch to the time

of CMB last scattering, this limit can not be compared simply with the BBN constraint. (2) The PMF affects BBN not only via the cosmic expansion rate but also changes in $e^\pm$ distribution function. Therefore, the correspondence of Eq. (1) is only an approximation even in the BBN epoch. Hence, a consistent calculation including various aspects of PMF effects [18] is necessary. (3) A rigorous calculation of the CMB including PMF effects is also required as suggested in Ref. [51].

In this paper, we show details of the collision term in the Boltzmann equation for nuclei during BBN and calculate the possible effects of a PMF on the nuclear distribution and resultant light-element abundances produced during BBN. First, it is shown that, under existing constraints on the possible amplitudes for the PMF, nuclei are predominantly affected by Coulomb scattering with $e^\pm$s, the momenta of which are regulated by the PMF if the field strength is as high as $\approx 10^{11}$ G. Second, from a numerical integration of the collision term from Coulomb scattering, it is seen that nuclei experience very frequent scatterings most of which result in energy shifts by only $\mathcal{O}(10^{-5})T$. Third, the effects on the nuclear distribution function from the introduction of a discretization of $e^\pm$ momenta is analyzed. It is confirmed that the Coulomb scattering does not lead to a significant change in the nuclear isotropy and energy distributions. Finally, using a toy model, we illustrate the possible effects of a hypothetical anisotropy in the nuclear distribution function on the light elements produced during BBN.

We note that the evaluation of the collision term in the Boltzmann equation, performed here, does not depend on whether the magnetic field is homogeneous or not, on all but the smallest scales. As noted below electrons and positrons significantly change their directions on very short timescales. This means that the mean free path is very short $O(10^{-7})$ cm. The corresponding comoving scale is only $O(10^2)$ cm. At each position of a nucleus, only the magnetic field amplitude over this small scale matters. If there is an inhomogeneity in the magnetic field over this or smaller scales, the formulation here may need modification. However, the current formulation is applicable for inhomogeneity over larger scales. The purpose of the current paper is the first evaluation of detailed statistical properties of the effect of Coulomb scattering on the nuclear distribution function. We then show that for a typical upper limit on the magnetic field amplitude during BBN, the effects of magnetic fields via changes in the electron and positron distribution functions are small enough. This means that even in a universe with a spatially inhomogeneous field strength, any deviation in the nuclear distribution from a Maxwell-Boltzmann form at any location can be safely neglected.

II. TIMESCALES

First, we show that during the BBN epoch at $T_9 = 1$, the motions of $e^\pm$s are controlled by the magnetic field if the

field is strong, i.e., $B \sim 10^{11}$ G, while the motion of nuclei is governed by Coulomb collisions with $e^{\pm}$s.

A. $e^{\pm}$

The gyrofrequency is a typical rate for the magnetic field effect on charged particles [54]. For $e^{\pm}$ it is given by

$$\omega_g = eB/E,$$
$$= 3.52 \times 10^{18} \text{ s}^{-1} \left(\frac{B}{10^{11} \text{ G}} \right) \left(\frac{E}{0.511 \text{ MeV}} \right)^{-1}, \quad (2)$$

where E is the energy of the $e^{\pm}$. Momentum exchange is dominated by Coulomb scatterings with abundant $e^{\pm}$s during BBN. The momentum transfer cross section is estimated as follows. As a rough approximation we consider scatterings off of target $e^{\pm}$ particles at rest in the frame of the cosmic fluid under the nonrelativistic approximation. The maximum impact parameter is set to the Debye length given by

$$b_{\max} = \lambda_D = 7.67 \times 10^{-9} \text{ cm} \quad (\text{at } T_9 = 1), \quad (3)$$

with

$$\lambda_D = \sqrt{T/(4\pi n_e e^2)}, \quad (4)$$

$$\approx \sqrt{\frac{\pi^{1/2}}{2^{5/2} \alpha m_e^{3/2} T^{1/2}}} e^{m_e/(2T)} \quad (\text{for } T \lesssim m_e), \quad (5)$$

where $n_e = n_{e^-} + n_{e^+}$ is the total number density of $e^{\pm}$, e and m_e are the electronic charge and mass, respectively, and $\alpha = e^2$ is the fine structure constant.

We use the relation between the scattering angle and the impact parameter,

$$b_{\max} = \frac{q_1 q_2 e^2}{m v^2} \cot \left(\frac{\theta_{\min}}{2} \right), \quad (6)$$

where q_1 and q_2 are charge numbers of reacting particles 1 and 2, respectively, $m = m_e/2$ is the reduced mass, v is the $e^{\pm}$ velocity, and $\theta_{\min}$ is the minimum scattering angle. Then, the maximum of $\mu \equiv \cos \theta$ at $T_9 = 1$ is given by

$$\mu_{\max} = \cos \theta_{\min},$$
$$\approx 1 - 1.08 \times 10^{-8} v^{-4}, \quad (7)$$

where a small angle approximation was adopted. With this maximum cosine $\mu_{\max}$, the momentum transfer cross section is given by

$$\sigma_{\mathrm{mt}}(\mu < \mu_{\max}) \approx \int_{-1}^{\mu_{\max}} \frac{d\sigma}{d\mu} \frac{\Delta q_e}{q_e} d\mu,$$
$$\approx 4.54/q_e^2, \quad (8)$$

where q_e and Δq_e are the initial momentum and the momentum transfer of $e^{\pm}$, respectively, and the differential Mott cross section is given by

$$\frac{d\sigma}{d\mu}(v, \mu) = \frac{2\pi\alpha^2}{v^2 q_e^2} \frac{1}{(1-\mu)^2} \left[1 - \frac{v^2}{2}(1-\mu) \right]. \quad (9)$$

The momentum transfer rate is then given by

$$\Gamma_{\mathrm{Coul}}(\mu < \mu_{\max}) \approx n_e \sigma_{\mathrm{mt}}(\mu < \mu_{\max}),$$
$$= 1.65 \times 10^{17} \text{ s}^{-1} v^{-2} \quad (\text{at } T_9 = 1). \quad (10)$$

The ratio of this scattering rate to the gyrofrequency is given by

$$R = \frac{\Gamma_{\mathrm{Coul}}(\mu < \mu_{\max})}{\omega_g},$$
$$\approx \frac{4.69 \times 10^{-2}}{v^2} \left(\frac{B}{10^{11} \text{ G}} \right)^{-1} \quad (\text{at } T_9 = 1). \quad (11)$$

For a large enough field strength of $B \sim 10^{11}$ G and $v \sim 1$, the Coulomb scattering rate is significantly smaller than the gyrofrequency. Therefore, the perturbation due to Coulomb scattering from the discretized momentum distribution would be small.

B. Nuclei

Scatterings are dominated by the Coulomb scattering with $e^{\pm}$. The maximum μ at $T_9 = 1$ is derived from Eq. (6) to be

$$\mu_{\max} = \cos \theta_{\min} \approx 1 - 2.70 \times 10^{-9} Z^2 v^{-4}, \quad (12)$$

where Z is the atomic number of the nucleus. The momentum transfer cross section is then given by

$$\sigma_{\mathrm{mt}}(\mu < \mu_{\max}) \approx \int_{-1}^{\mu_{\max}} \frac{d\sigma}{d\mu} \frac{\Delta q_e}{q_e} \frac{q_e}{q_A} d\mu,$$
$$\approx 18.2/(Z q_e q_A), \quad (13)$$

where q_A is the nuclear momentum. Accordingly, the momentum transfer rate is given by

$$\Gamma_{\mathrm{Coul}}(\mu < \mu_{\max}) \approx n_e \sigma_{\mathrm{mt}}(\mu < \mu_{\max}),$$
$$= \frac{2.17 \times 10^{16} \text{ s}^{-1}}{Z A^{1/2} v} \quad (\text{at } T_9 = 1), \quad (14)$$

where A is the nuclear mass number.

The ratio of this scattering rate to the gyrofrequency [Eq. (2)] is given by

$$R = \frac{\Gamma_{\text{Coul}}(\mu < \mu_{\text{max}})}{\omega_g} \tag{15}$$

$$\sim \frac{6.15 \times 10^4}{v} \frac{A^{1/2}}{Z^2} \left(\frac{E_A}{3\text{GK}/2}\right)^{-1/2} \left(\frac{T}{m_e}\right)^{3/2}$$

$$\times \exp\left(-m_e/T\right) \left(\frac{B}{10^{11}\,\text{G}}\right)^{-1}, \tag{16}$$

$$= \frac{11.3}{v} \frac{A^{1/2}}{Z^2} \left(\frac{B}{10^{11}\,\text{G}}\right)^{-1} \quad (\text{at } T_9 = 1). \tag{17}$$

For a large enough field strength, $B \sim 10^{11}$ G, the Coulomb scattering rate is large enough when $T \sim m_e$, but diminishes relative to the gyrofrequency at lower temperatures. Since this ratio is larger than that of $e^{\pm}$ at $T_9 = 1$, we can expect situations in which the distribution of $e^{\pm}$ is predominantly governed by the magnetic field while those of nuclei are determined by Coulomb collisions with $e^{\pm}$ in the BBN epoch.

III. MODEL

Under the assumption of a homogeneous distribution of nonrelativistic nuclei during BBN, the invariant Boltzmann equation for nuclei in the $e^{\pm}$ plasma has the form of

$$\frac{\partial f_A}{\partial t} + e(\boldsymbol{v} \times \boldsymbol{B})^i \frac{\partial f_A}{\partial p_A^i}$$

$$= \frac{m_A}{E_A} \frac{g_e}{(2\pi\hbar)^3} \int d^3 q_e \frac{E_e^{(\text{lab})}}{E_e} \int d\Omega_{\text{nuc}} v \frac{d\sigma}{d\Omega_{\text{nuc}}}$$

$$\times [f_A' f_e' (1 \pm f_A)(1 - f_e) - f_A f_e (1 \pm f_A')(1 - f_e')], \tag{18}$$

where $g_e = 4$ is the sum of the statistical degrees of freedom of e^- and e^+, m_A is the nuclear mass, E_e is the electron energy, f_A and f_A' are the distribution functions of nuclear momenta in the initial and final states, $\boldsymbol{p}_A$ and $\boldsymbol{p}_A'$, respectively, and f_e and f_e' are the distribution functions of $e^{\pm}$ momenta in the initial and final states, $\boldsymbol{q}_e$ and $\boldsymbol{q}_e'$, respectively. The relative velocity $v(\boldsymbol{p}_A, \boldsymbol{q}_e)$ is equal to the electron velocity in the nuclear rest frame. The quantity $d\sigma/d\Omega_{\text{nuc}}$ is the differential Mott cross section with Ω_{nuc} the solid angle in the nuclear rest frame, and the $E_e^{(\text{lab})}$ is the electron energy in the nuclear rest frame.

We take the z axis as the field direction in a small local domain. The second term on the left-hand side is zero if the gradient of the distribution function is proportional to the momentum along a plane perpendicular to the z axis, i.e., $\partial f_A/\partial p_{Ai} \propto p_{Ai}$ for $i = x$ and y. We assume that the second term is zero hereafter. On the right-hand side, the first and second terms correspond to the production and destruction, respectively, from Coulomb scattering.

When f_e and f_e' obey an FD distribution, the quantity in the square brackets becomes zero for FD or BE distributions for nucleus A. Therefore, an FD or BE distribution is a trivial steady-state solution of the Boltzmann equation, and at BBN temperatures, both of them are well approximated by an MB distribution, i.e.,

$$f_{\text{MB}}(\boldsymbol{p}_A) = n_A (2\pi m_A T)^{-3/2} \exp\left[-p_A^2/(2m_A T)\right], \tag{19}$$

where n_A is the number density of the nuclide A and $p_A = |\boldsymbol{p}_A|$.

A. $B = 0$ case

When there is no magnetic field, $e^{\pm}$s are assumed to have an FD distribution. Then, the production and destruction terms exactly cancel with each other. The destruction term is described by

$$\frac{df_A}{dt}\bigg|_{\text{des}} (p_A; 0) = -f_A(p_A) \int dq_e \frac{q_e^2}{E_e(q_e)} f_e(q_e)$$

$$\times \int d\Xi E_e^{(\text{lab})}(p_A, q_e, \Xi) v(p_A, q_e, \Xi)$$

$$\times \int_{-1}^{\mu_{\text{max}}(p_A, \Theta; q_e)} d\mu \frac{d\sigma(v, \mu)}{d\mu} \frac{1}{2\pi}$$

$$\times \int_0^{2\pi} d\phi \{1 - f_e'(q_e'[p_A, q_e, \Xi, \mu, \phi])\}, \tag{20}$$

where $\mu_{\text{max}}(p_A, \Theta; q_e)$ is the maximum μ value as a function of p_A and the angle between $\boldsymbol{p}_A$ and $\boldsymbol{q}_e$, i.e., Θ, for a fixed $q_e = |\boldsymbol{q}_e|$. The parameter $\Xi = \cos\Theta$, and ϕ is the azimuthal angle at the scattering. The term $[1 - f_e'(q_e')]$ is from the Pauli blocking of $e^{\pm}$ with $\boldsymbol{q}_e' = \boldsymbol{h}(\boldsymbol{p}_A, \boldsymbol{q}_e, \mu, \phi)$ the momentum vector of $e^{\pm}$ in the final state. The quantity $q_e^{\text{nuc}}(q_e, p_A, \Theta)$ is the electron momentum in the nuclear rest frame, which appears in the differential Mott cross section. Note that when $\boldsymbol{p}_A, \boldsymbol{q}_e$, and (μ, ϕ) are given, $\boldsymbol{p}_A'$ and $\boldsymbol{q}_e'$ are determined.

In the BBN epoch, the $e^{\pm}$ plasma has an FD distribution when there is no magnetic field, i.e., $f_{e\mp}(\boldsymbol{q}_e) = 1/\{\exp[(E_e \mp \mu_e)/T] + 1\}$ with $E_e = \sqrt{m_e^2 + q_e^2}$ the total energy. Unless $T \ll m_e$, the electron chemical potential is negligible, and we use the same function $f_e(\boldsymbol{q}_e)$ for $e^{\pm}$s.

The upper limit on the integral, i.e., $\mu_{\text{max}}(p_A, \Theta; q_e)$ appears because of the minimum scattering angle θ_{min}. The minimum angle is set so that the Mott scattering is ineffective if the impact parameter is larger than the Debye screening length. The effective minimum scattering angle is then given by

$$\theta_{\text{min}} = 2\tan^{-1}\left\{\alpha\omega_{\text{p}}/[(m_e T)^{1/2} v^2]\right\}, \tag{21}$$

where $\omega_{\text{p}} = 4\pi\alpha n_e/m_e$ is the plasma frequency of the background $e^{\pm}$ plasma.

B. $B \neq 0$ case

We estimate the maximum possible effect of the B field on nuclear distribution functions assuming that $e^\pm$s in their initial states only have a discretized momentum distribution. An upper limit on the magnetic field strength is adopted from BBN studies with a PMF [18].

We assume some mechanism which only modifies the initial state momentum distribution of $e^\pm$s, such as a PMF. An extreme case is considered here that the initial state energy spectrum is completely discretized into Landau levels. The Pauli blocking for $e^\pm$ is negligible since the initial momentum of the $e^\pm$ is discretized and the final momentum is continuous in the present application. Since most scatterings result in small Δq_e (see below), transitions to different n states are less important. Therefore, the Pauli blocking effect is neglected in this case.

For the case of a finite B field, the destruction term in the Boltzmann equation is described by

$$\frac{df_A}{dt}\bigg|_{\text{des}}(p_A; B) = -\frac{m_A}{E_A}\frac{g_e}{(2\pi\hbar)^3}f_A(\boldsymbol{p}_A)eB\int_{-\infty}^{\infty}dq_{e\parallel}\int d\phi_2$$

$$\times \sum_{n=0}^{\infty}\frac{(2-\delta_{n0})}{2}\frac{E_e^{(\text{lab})}(p_A, q_e, \Xi)}{E_e(q_e)}$$

$$\times f_{en}(q_{e\parallel}; T)v(p_A, q_e, \Xi)\sigma_{\text{tot}}(v), \quad (22)$$

$$f_{en}(q_{e\parallel}; T) = \{1 + \exp[E_n(q_z)/T]\}^{-1}, \quad (23)$$

where $q_e = (q_{e\perp}^2 + q_{e\parallel}^2)^{1/2}$ with $q_{e\perp}^2 = 2neB$ and $E_n = (q_e^2 + m_e^2)^{1/2}$ are the momentum and energy of the nth Landau level, δ_{n0} is the Kronecker delta, and σ_{tot} is the total cross section for Coulomb scattering.

In the coordinates of $\boldsymbol{p}_A = p_A(\sin\theta_1, 0, \cos\theta_1)$ and $\boldsymbol{q}_e = q_e(\sin\theta_2\cos\phi_2, \sin\theta_2\sin\phi_2, \cos\theta_2)$, it follows that

$$\Xi = \sin\theta_1\sin\theta_2\cos\phi_2 + \cos\theta_1\cos\theta_2. \quad (24)$$

IV. RESULTS

Figure 1 shows the differential rate of change of the distribution function $f(\boldsymbol{p}_A)$ with respect to the final state momentum $\boldsymbol{p}'_A$, i.e., $\partial^2 f(\boldsymbol{p}_A, \boldsymbol{p}'_A)/(\partial t\partial p'_A)$, as a function of the change of the proton energy $\Delta E_A/T$ for $p + e^\pm \to p + e^\pm$ scattering in the case of $B = 0$. The central region of small $|\Delta E_A/T|$ has maximum rates since the small energy changes that result from small angle scatterings have a huge cross section as long as the angle is above the lower limit. When the amplitude $|\Delta E_A/T|$ is larger, large angle scatterings are required. Since they occur with smaller differential cross sections, the rates are also smaller.

It is observed that the differential collision term has a plateau at $\sim 10^3 f$ GeV^2 in the region of $|\Delta E_A/T| \lesssim 10^{-5}$. The typical width of the distribution is rather consistent with the following analytical estimate. The largest
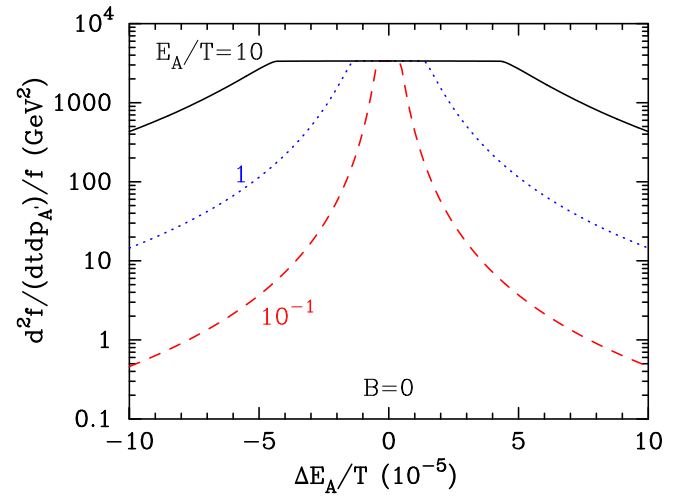

FIG. 1. Differential destruction term of the Boltzmann equation as a function of the change of the proton energy due to a scattering, for initial proton energies of $E_A/T = 10^{-1}$, 1, and 10 at $T = 10^9$ K in the case of no magnetic field.

contribution to the collision integral comes from the parameter region with the smallest possible scattering angle for the thermal energy of the $e^\pm$. The minimum scattering angle for the thermal energy is given [Eq. (21)] by

$$\theta_{\text{min}} \approx 8.5 \times 10^{-5}\left(\frac{\omega_p}{1.22 \times 10^{-6}\text{ GeV}}\right)T_9^{-1/2}v^{-2}. \quad (25)$$

For $p_A \gg q_e$ as in the case of thermal nuclei during the BBN epoch, we adopt an approximation that the Lorentz gamma for the nuclear velocity is $\gamma_A = (1 - v_A^2)^{-1/2} \approx 1$, $q_e^{\text{nuc}} \approx q_e$, and the angle of $\boldsymbol{q}_e^{\text{nuc}}$ measured from the direction of $\boldsymbol{p}_A$, $\Theta' \approx \Theta$. Then it follows that $\Delta p_A^2 \sim p_A q_e\theta$. For this value, the change in the nuclear energy for $E_e/T \sim 1$ has a typical value of

$$\frac{|\Delta E_A|}{T} \approx 10^{-6}\sqrt{\frac{E_A}{T}}A^{-1}\left(\frac{\theta}{10^{-4}}\right). \quad (26)$$

The upper panel in Fig. 2 shows the change in the destruction term of the Boltzmann equation for protons as a function of $\mu_1 = \cos\theta_1$, i.e., $\Delta df/dt(\mu_1)/[(1/2)\int d\mu_1 df/dt(\mu_1)]$, at $T = 10^9$ K for $B = 2.0 \times 10^{11}$ G. The thin three lines near zero are differences in the total destruction rates. It is confirmed that the proton distribution function is independent of the direction even if the isotropy of the $e^\pm$ momentum is broken in a magnetic field. Also plotted are thick lines for the partial destruction rate by $e^\pm$ particles moving toward the hemisphere of $q_{e\parallel} > 0$. At high energies relevant to nuclear reactions, a significant dependence on μ_1 is seen (thick solid line for $E_A/T = 20$). The partial destruction rate is smaller at larger μ_1 since the
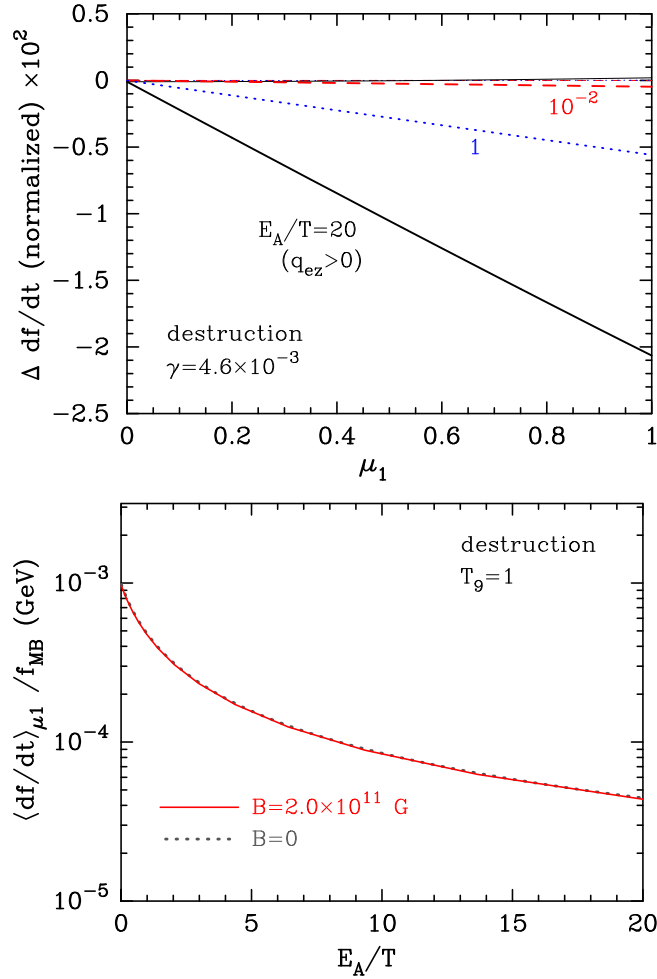
FIG. 2. Upper panel: difference of the destruction term of the Boltzmann equation for protons as a function of the angle between the proton momentum and the magnetic field at $T = 10^9$ K. The field is the largest allowed value, 2.0×10^{11} G. Thin three lines show differences in the total destruction rate although they are nearly indistinguishable. The sloping three thick lines show differences in the partial destruction rate by $e^\pm$ particles with $q_{e\parallel} > 0$. Lower panel: the destruction term averaged over the direction of the proton as a function of proton energy at $T = 10^9$ K. Solid and dotted lines correspond to the results for $B = 2.0 \times 10^{11}$ G and 0, respectively.

FIG. 3. Primordial abundances as a function of the anisotropy parameter a (open circles). Y_p is the mass fraction of ^{4}He. Solid lines connect the calculated total abundances, while the dashed and dotted lines correspond to separated yields of ^{7}Be and ^{7}Li in BBN, respectively. Boxes roughly indicate values of the anisotropy parameter where the observational constraints are satisfied.

electron momentum in the nuclear rest frame is smaller than that in the fluid rest frame. However, after integration over the full phase space of $\boldsymbol{q}_e$, the dependence of the destruction rate on μ_1 diminishes (thin horizontal lines).

The lower panel in Fig. 2 shows the destruction term averaged over the proton direction, i.e., $\langle df/dt \rangle_{\mu_1} = \int d\mu_1 df/dt(\mu_1)/2$, as a function of the proton energy. Solid and dotted lines correspond to the results for $B = 2.0 \times 10^{11}$ G and 0, respectively. There is no significant difference, and it is also confirmed that the magnetic field does not affect the proton energy distribution. Note that, although the total $e^\pm$ number density is different from that
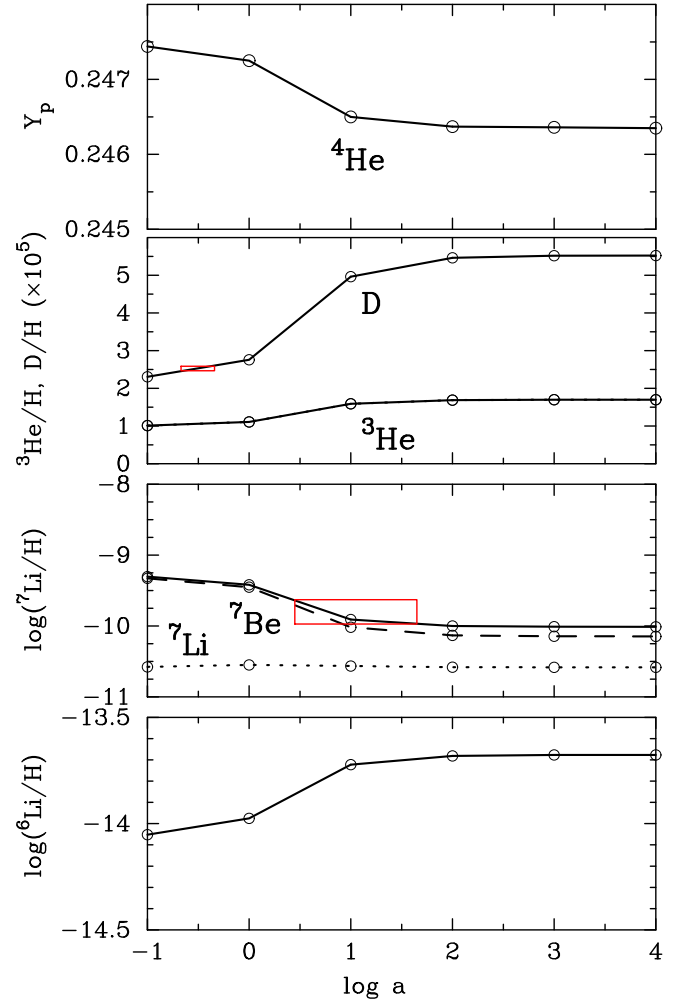
of a MB distribution in a magnetic field [19], the difference is small for the upper bound on the field strength adopted here.

V. CONSTRAINT ON ANISOTROPY

We derive a constraint on anisotropy in the nuclear momentum distribution during BBN. In this case, modifications to the MB distribution can be formulated as a change in the effective relative velocity distribution. Similarly to a deviation of the energy spectrum [11,12], an introduction of anisotropy affects nucleosynthesis. As an example, we assume that the densities of particles moving in some special direction are enhanced, as described by $f_a(\boldsymbol{v}_i) \propto g_a(\mu_i) \equiv (1 + a\mu_i)$ [for $\mu_i \equiv \boldsymbol{v}_i \cdot \boldsymbol{B}/(v_i B) > -1/a$] and 0 (otherwise). Similar to Ref. [13], the relative velocity distribution function can then be written as

$$f_{a}^{\text{rel}}(\boldsymbol{v}) = \int_{0}^{2\pi} d\phi_{\text{CM}} \int_{-1}^{1} d\mu_{\text{CM}} \int_{0}^{\infty} V^2 dV f_a(\boldsymbol{v}_A) f_a(\boldsymbol{v}_e),$$

$$= B_1(a)^2 \frac{(m_1 m_2)^{3/2}}{(2\pi T)^3} \exp\left[-\frac{\mu v^2}{2T}\right]$$

$$\times \int_{0}^{\infty} V^2 dV \exp\left[-\frac{MV^2}{2T}\right] \int_{0}^{2\pi} d\phi_{\text{CM}}$$

$$\times \int_{-1}^{1} d\mu_{\text{CM}} g_a(\mu_1) g_a(\mu_2), \qquad (27)$$

where $B_1(0 \leq a \leq 1) = 1$ and $B_1(a > 1) = 2/[1 + a/2 + 1/(2a)]$ are the normalization constants, m_1 and m_2 are masses of reacting particles 1 and 2, $M = m_1 + m_2$, V is the center of mass (CM) velocity, while μ_{CM} and ϕ_{CM} are, respectively, the cosine of the polar angle and azimuthal angle at the scattering.

Figure 3 shows light element abundances as a function of the anisotropy parameter a in the BBN model including the anisotropy in all nuclear distribution functions. The introduction of this type of anisotropy causes larger energies of the CM, i.e., $MV^2/2$, and smaller relative energies in the CM system, i.e., $E = \mu v^2/2$. As a result, a larger a leads to a softer distribution of E with a smaller average. Then, nuclear reaction rates are hindered and light element abundances are changed in a similar manner as in the case where the isotropic distribution function deviates from a MB distribution to the softer side. The dependencies of abundances on anisotropy is very similar to those of a spectral distortion [12,13].

VI. SUMMARY

The effect of Landau discretization of the $e^{\pm}$ momenta on the collision term of protons during BBN was studied. At $T = 10^9$ K, nuclei experience $\sim 10^{21}$ scatterings per second from $e^{\pm}$, and most of the scatterings lead to small, $\mathcal{O}(1)$ eV, changes of the nuclear kinetic energy. When the magnetic field amplitude is set to the largest value allowed by observations, the $e^{\pm}$ distribution experiencing the magnetic field does not lead to any significant directional dependence in the collisional destruction term of nuclei. A constraint on the amplitude of anisotropies in the nuclear distribution function during BBN was also derived.

[1] V. T. Voronchev, Y. Nakao, and M. Nakamura, Non-thermal processes in standard big bang nucleosynthesis. I: In-flight nuclear reactions induced by energetic protons, J. Cosmol. Astropart. Phys. 05 (2008) 010.

[2] N. Sasankan, A. Kedia, M. Kusakabe, and G. J. Mathews, Analysis of the multi-component relativistic Boltzmann equation for electron scattering in big bang nucleosynthesis, Phys. Rev. D **101**, 123532 (2020).

[3] C. Hayashi and M. Nishida, Formation of light nuclei in the expanding Universe, Prog. Theor. Phys. **16**, 613 (1956).

[4] R. V. Wagoner, W. A. Fowler, and F. Hoyle, On the synthesis of elements at very high temperatures, Astrophys. J. **148**, 3 (1967).

[5] A. Kedia, N. Sasankan, G. J. Mathews, and M. Kusakabe, Simulations of multicomponent relativistic thermalization, Phys. Rev. E **103**, 032101 (2021).

[6] S. D. McDermott and M. S. Turner, Nuclear kinetic equilibrium during big bang nucleosynthesis, arXiv:1811.04932.

[7] D. Lindley, Radiative decay of massive neutrinos and cosmic element abundances., Mon. Not. R. Astron. Soc. **188**, 15P (1979).

[8] M. H. Reno and D. Seckel, Primordial nucleosynthesis: The effects of injecting hadrons, Phys. Rev. D **37**, 3441 (1988).

[9] S. Dimopoulos, R. Esmailzadeh, L. J. Hall, and G. D. Starkman, Is the Universe closed by baryons? Nucleosynthesis with a late-decaying massive particle, Astrophys. J. **330**, 545 (1988).

[10] C. Tsallis, Possible generalization of Boltzmann-Gibbs statistics, J. Stat. Phys. **52**, 479 (1988).

[11] C. Bertulani, J. Fuqua, and M. Hussein, Big bang nucleosynthesis with a non-Maxwellian distribution, Astrophys. J. **767**, 67 (2013).

[12] S. Hou, J. He, A. Parikh, D. Kahl, C. Bertulani, T. Kajino, G. Mathews, and G. Zhao, Non-extensive statistics to the cosmological lithium problem, Astrophys. J. **834**, 165 (2017).

[13] M. Kusakabe, T. Kajino, G. J. Mathews, and Y. Luo, On the relative velocity distribution for general statistics and an application to big-bang nucleosynthesis under Tsallis statistics, Phys. Rev. D **99**, 043505 (2019).

[14] T. D. Rueter, T. G. Rizzo, and J. L. Hewett, Dark matter freeze out with tsallis statistics in the early Universe, arXiv:1911.11254.

[15] R. F. O'Connell and J. J. Matese, Effect of a constant magnetic field on the neutron beta decay rate and its astrophysical implications, Nature (London) **222**, 649 (1969).

[16] B.-l. Cheng, A. V. Olinto, D. N. Schramm, and J. W. Truran, Constraints on the strength of primordial magnetic fields from big bang nucleosynthesis revisited, Phys. Rev. D **54,** 4714 (1996).

[17] Y. Luo, M. A. Famiano, T. Kajino, M. Kusakabe, and A. B. Balantekin, Screening corrections to electron capture rates and resulting constraints on primordial magnetic fields, Phys. Rev. D **101,** 083010 (2020).

[18] M. Kawasaki and M. Kusakabe, Updated constraint on a primordial magnetic field during big bang nucleosynthesis and a formulation of field effects, Phys. Rev. D **86,** 063003 (2012).

[19] P. J. Kernan, G. D. Starkman, and T. Vachaspati, Big bang nucleosynthesis constraints on primordial magnetic fields, Phys. Rev. D **54,** 7207 (1996).

[20] G. Greenstein, Primordial helium production in "Magnetic" cosmologies, Nature (London) **223,** 938 (1969).

[21] Y. Luo, T. Kajino, M. Kusakabe, and G. J. Mathews, Big bang nucleosynthesis with an inhomogeneous primordial magnetic field strength, Astrophys. J. **872,** 172 (2019).

[22] T. Vachaspati, Progress on cosmological magnetic fields, Rep. Prog. Phys. **84,** 074901 (2021).

[23] A. D. Dolgov and D. Grasso, Generation of Cosmic Magnetic Fields and Gravitational Waves at Neutrino Decoupling, Phys. Rev. Lett. **88,** 011301 (2001).

[24] A. Brandenburg and W. H. Matthaeus, Magnetic helicity evolution in a periodic domain with imposed field, Phys. Rev. E **69,** 056407 (2004).

[25] R. Banerjee and K. Jedamzik, The evolution of cosmic magnetic fields: From the very early Universe, to recombination, to the present, Phys. Rev. D **70,** 123003 (2004).

[26] L. M. Widrow, D. Ryu, D. R. Schleicher, K. Subramanian, C. G. Tsagas, and R. A. Treumann, The first magnetic fields, Space Sci. Rev. **166,** 37 (2012).

[27] A. Brandenburg, R. Durrer, Y. Huang, T. Kahniashvili, S. Mandal, and S. Mukohyama, Primordial magnetic helicity evolution with a homogeneous magnetic field from inflation, Phys. Rev. D **102,** 023536 (2020).

[28] S. Hutschenreuter, S. Dorn, J. Jasche, F. Vazza, D. Paoletti, G. Lavaux, and T. A. Enßlin, The primordial magnetic field in our cosmic backyard, Classical Quantum Gravity **35,** 154001 (2018).

[29] M. Sanati, Y. Revaz, J. Schober, K. E. Kunze, and P. Jablonka, Constraining the primordial magnetic field with dwarf galaxy simulations, Astron. Astrophys. **643,** A54 (2020).

[30] F. Vazza, D. Paoletti, S. Banfi, F. Finelli, C. Gheller, S. P. O'Sullivan, and M. Brüggen, Simulations and observational tests of primordial magnetic fields from cosmic microwave background constraintsok, Mon. Not. R. Astron. Soc. **500,** 5350 (2020).

[31] H. Katz et al., Introducing SPHINX-MHD: The impact of primordial magnetic fields on the first galaxies, reionization, and the global 21 cm signal, arXiv:2101.11624.

[32] B. Ratra, Cosmological "Seed" magnetic field from inflation, Astrophys. J. Lett. **391,** L1 (1992).

[33] A. Zucca, Y. Li, and L. Pogosian, Constraints on primordial magnetic fields from planck combined with the south pole telescope CMB B-mode polarization measurements, Phys. Rev. D **95,** 063506 (2017).

[34] P. A. R. Ade et al. (BICEP2, Keck Arrary Collaboration), BICEP2 / Keck Array IX: New bounds on anisotropies of CMB polarization rotation and implications for axionlike particles and primordial magnetic fields, Phys. Rev. D **96,** 102003 (2017).

[35] D. R. Sutton, C. Feng, and C. L. Reichardt, Current and future constraints on primordial magnetic fields, Astrophys. J. **846,** 164 (2017).

[36] L. Pogosian and A. Zucca, Searching for primordial magnetic fields with CMB B-modes, Classical Quantum Gravity **35,** 124004 (2018).

[37] D. G. Yamazaki, Impact of a primordial magnetic field on cosmic microwave background B modes with weak lensing, Phys. Rev. D **97,** 103525 (2018).

[38] D. Paoletti, J. Chluba, F. Finelli, and J. A. Rubino-Martin, Improved CMB anisotropy constraints on primordial magnetic fields from the post-recombination ionization history, Mon. Not. R. Astron. Soc. **484,** 185 (2019).

[39] T. Minoda, K. Ichiki, and H. Tashiro, Small-scale CMB anisotropies induced by the primordial magnetic fields, J. Cosmol. Astropart. Phys. 03 (**2021**) 093.

[40] D. Paoletti and F. Finelli, Constraints on primordial magnetic fields from magnetically-induced perturbations: Current status and future perspectives with LiteBIRD and future ground based experiments, J. Cosmol. Astropart. Phys. 11 (2019) 028.

[41] T. Minoda, H. Tashiro, and T. Takahashi, Insight into primordial magnetic fields from 21-cm line observation with EDGES experiment, Mon. Not. R. Astron. Soc. **488,** 2001 (2019).

[42] P. K. Natwariya, Constraint on primordial magnetic fields in the light of ARCADE 2 and EDGES observations, Eur. Phys. J. C **81,** 394 (2021).

[43] A. Bera, K. K. Datta, and S. Samui, Primordial magnetic fields during the cosmic dawn in light of EDGES 21-cm signal, Mon. Not. R. Astron. Soc. **498,** 918 (2020).

[44] M. Safarzadeh and A. Loeb, An upper limit on primordial magnetic fields from ultra-faint dwarf galaxies, Astrophys. J. Lett. **877,** L27 (2019).

[45] S. Saga, H. Tashiro, and S. Yokoyama, Limits on primordial magnetic fields from direct detection experiments of gravitational wave background, Phys. Rev. D **98,** 083518 (2018).

[46] M. Kusakabe and M. Kawasaki, Chemical separation of primordial Li$^+$ during structure formation caused by nanogauss magnetic field, Mon. Not. R. Astron. Soc. **446,** 1597 (2015).

[47] M. Kusakabe and M. Kawasaki, Initial Li abundances in the proto-galaxy and globular clusters based upon the chemical separation and hierarchical structure formation, Astrophys. J. Lett. **876,** L30 (2019).

[48] F. Spite and M. Spite, Abundance of lithium in unevolved halo stars and old disk stars: Interpretation and consequences, Astron. Astrophys. **115,** 357 (1982), http://adsabs.harvard.edu/pdf/1982A&A...115..357S.

[49] L. Sbordone et al., The metal-poor end of the Spite plateau. 1: Stellar parameters, metallicities and lithium abundances, Astron. Astrophys. **522,** A26 (2010).

[50] S. Hayakawa et al., Constraining the primordial lithium abundance: New cross section measurement of the 7Be + n reactions updates the total 7Be destruction rate, Astrophys. J. Lett. **915,** L13 (2021).

[51] K. Jedamzik and L. Pogosian, Relieving the Hubble Tension with Primordial Magnetic Fields, Phys. Rev. Lett. **125,** 181302 (2020).

[52] M. J. Reid, D. W. Pesce, and A. G. Riess, An improved distance to NGC 4258 and its implications for the Hubble constant, Astrophys. J. Lett. **886,** L27 (2019).

[53] N. Aghanim *et al.* (Planck Collaboration), Planck 2018 results. VI. Cosmological parameters, Astron. Astrophys. **641,** A6 (2020).

[54] J. D. Jackson, *Classical Electrodynamics* (John Wiley & Sons, New York, 1975).